KSCE Journal of Civil Engineering (2020) 24(12):3692-3702
DOI 10.1007/s12205-020-0441-3

pISSN 1226-7988, eISSN 1976-3808
www.springer.com/12205

Hydraulic Engineering

Flow Downstream Sluice Gate with Orifice

Ibrahim M. Mohamed[a] **and Fahmy S. Abdelhaleem**[b]

[a]*Shoubra Faculty of Engineering, Benha University, Shoubra 11626, Egypt*
[b]*Benha Faculty of Engineering, Benha University, Benha 13512, Egypt*

ARTICLE HISTORY

Received 11 March 2020
Revised 8 June 2020
Accepted 14 July 2020
Published Online 24 September 2020

KEYWORDS

Sluice gate
Gate opening
Orifice
Discharge coefficient
Scour depth
Hydraulic jump
Energy dissipation

ABSTRACT

Gates and orifices were significant common structures used in controlling and adjusting the flow in water system channels. Installing of an orifice with sluice gates, increase the flow discharge with minimizing the horizontal jets under gate that was attributed with higher bed flow velocity and larger scour geometry downstream these gates. An experimental study was conducted to examine the flow pattern and the bed configurations downstream sluice gates with an orifice. In this research, a circular orifice employed with sluice gates as a means of energy dissipation downstream the gates, was explored. Forty-five runs were completed under 3 discharges, 3 upstream water heads, and 7 tail gate water depths. Five models for sluice gate with orifice were utilized. A series of regime plots were created to help designing the sluice gate with orifice as heading up and flow distributions structures. The outcomes illustrated that combining of an orifice with sluice gates productively scattered the jump energy and diminished the downstream local scour compared to the conventional sluice gate. Additionally, existed equations used to predict the jump length downstream sluice gate were applicable in case of sluice gate with orifice provided similar flow conditions were achieved. The optimum ratio of orifice and under gate areas was also introduced.

1. Introduction

Discharge can advantageously be estimated by hydraulic structures for controlling discharge and water depth, as they made a coordinated connection between depth and discharge. Orifices and sluice gate were normally utilized flow control and metering devices. The sluice gate was a hydraulic structure utilized for this reason which enabled the flow to go underneath. Downstream free flow happened at a (moderately) huge proportion of upstream depth to the gate opening height. However, submerged flow at the downstream would happen for low estimations of this proportion. For an openly giving flow underneath a sluice gate, the water surface was very smooth while for a submerged flow, the comparing flow profile was amazingly harsh. With respect to flow under a sluice gate and the flow pattern at downstream including the discharge coefficient and the water jump as a hydraulic phenomenon, numerous works have been reported, for example, by Rajaratnam and Subramanya (1967) carried out experimental model to develop a general equation for prediction flow downstream sluice gate. Rajaratnam (1977) concluded that the water surface profile underneath sluice gate installed in rectangular channel was similar.

USBR (1955), Douma (2017), and Safranez (2017) estimated the jump length (L_j) downstream sluice gate in rectangular channel in terms of sequent depth (y_2) as presented in Eqs. (1), (2), and (3), respectively:

$$L_j = 6.0y_2\,, \tag{1}$$

$$L_j = 5.2y_2\,, \tag{2}$$

$$L_j = 3.0y_2\,. \tag{3}$$

Silvester (1964), Hager (1992), Chertoussov (2017) developed developed relation between the jump length (L_j), initial flow depth at the jump (y_1), and the Froude No. at the initial depth (F_{r1}). Their formulas were presented in Eqs. (4), (5), and (6), respectively:

$$\frac{L_j}{y_1} = 220\tanh\left(\frac{F_{r1}-1}{22}\right), \tag{4}$$

$$L_j = 10.3y_1(F_{r1}-1)^{0.81}\,, \tag{5}$$

$$\frac{L_j}{y_1} = 9.75(F_{r1}-1)^{1.01}\,. \tag{6}$$

CORRESPONDENCE Ibrahim M. Mohamed mohamed.ibrahim@feng.bu.edu.eg Shoubra Faculty of Engineering, Benha University, Shoubra 11626, Egypt

Karbasi (2016) defined the jump length in terms of initial and sequent depths and the Froude No. at the initial depth, Eq. (7):

$$\frac{L_j}{y_1} = 3.987 F_{r1}^{-1.9951} \left(\frac{y_2}{y_1}\right)^{2.9081} . \tag{7}$$

Gupta et al. (2013) considered Reynolds number at the initial depth (R_{e1}) in the estimation of jump length and developed Eq. (8):

$$\frac{L_j}{y_1} = 4769.1 \left[\frac{F_{r1}^{2.1}}{R_{e1}}\right] + 25.064 . \tag{8}$$

Some researchers defined the jump length in the presence of hydraulic jump length coefficient (C_j) as in Eq. (9):

$$L_j = C_j (y_2 - y_1) . \tag{9}$$

Bambang and Lalu (2017), Ivanchenko (2017), Woycicki (2017), and Wu (2017) estimated the jump length coefficient (C_j) as presented in Eqs. (10), (11), (12), and (13), respectively:

$$C_j = 10 F_{r1}^{-0.16} , \tag{10}$$

$$C_j = 8 - 0.05 \left(\frac{y_2}{y_1}\right) , \tag{11}$$

$$C_j = 10.6 (F_{r1}^2)^{-0.185} , \tag{12}$$

$$C_j = 3.8274 + 3.0083 \left(\frac{y_1}{y_2}\right)^{0.1} . \tag{13}$$

Nasrin et al. (2017) developed Eq. (14) to relate the jump length to divergence ratio of wall and roughness elements height:

$$\frac{L_j}{y_1} = 8.924 F_{r1} + 11.473 B' - 12.390 \left(\frac{r}{y_1}\right) - 21.541 , \tag{14}$$

where the B' is the ratio between the width of stilling basin at upstream and downstream sides, and r is the height of roughness elements.

Carollo et al. (2009) applied dimensional analysis to develop functional relationship between the ratios for the sequent depth in hydraulic jump over rough and smooth beds. McCorquodale and Khalifa (1983) developed mathematical model for prediction the internal characteristics of the hydraulic jump including both roller and jump lengths in addition the velocity distribution. Leutheusser and Kartha (1972), studied experimentally and analytically the horizontal jump in smooth walled rectangular section, also they developed relationship between sequent depth ratio and the Froude numbers.

Accentuating the discharge coefficient of sluice gate (Carlos et al., 2009) commented that when the gate discharge data were unobtainable, the use of a contraction value of 0.611 for submerged sluice gates gave exceptional results (Henderson, 1966; Rajaratnam and Subramanya, 1967; Swamee, 1992; Garbrecht, 1977; Navid and Farzin, 2012) concluded that the discharge coefficient for vertical sluice gate depended on hydraulic and geometric parameters. They derived equations for the discharge coefficient that presented in Eqs. (15) – (19), respectively:

$$C_d = 0.0297 \left(\frac{G}{H}\right) + 0.589 , \tag{15}$$

$$C_d = 0.44457 \left(\frac{G}{H}\right)^{0.1219} , \tag{16}$$

$$C_d = 0.611 \left(\frac{H - G}{H + 15G}\right)^{0.072} , \tag{17}$$

$$C_d = 0.635 \sqrt{1 - \left(\frac{y_1}{H}\right)} , \tag{18}$$

$$C_d = \frac{\left(\frac{y_1}{G}\right)}{\sqrt{1 + \left(\frac{y_1}{H}\right)}} , \tag{19}$$

at which C_d: the discharge coefficient; y_1: the hydraulic jump initial depth; G: the height of gate opening; and H: the upstream head.

Barely any investigations were accessible about the utilization of these combined devices for flow measurements before (Majcherek, 1984) where the main thought of simultaneous flow over the weir and under the gate was presented.

Negm (1996), Delwar (1999), Negm et al. (2002), Jamal and Mehdi (2009) underscored the discharge prediction for the flow over traditional rectangular weirs and underneath gate. The outcomes reasoned that the upstream water head and the vertical distance between the weir base and the gate crest were the predominant parameters influencing the discharge (Negm et al., 1994; Alhamid et al., 1996) exhibited the characteristics of the instantaneous flow over rectangular weirs and under reversed triangular gate. Alhamid (Alhamid, 1999; Negm, 2002) created non-dimensional discharge equation for the flow through combined V-notch-gate device (Alhamid et al., 1997; Hayawi et al., 2008). featured the flow characteristics over a self-cleaning device for momentary flow over triangular weir and below a rectangular gate. The outcomes underscored that the impact of weir angle significantly affects the downstream flow pattern where the greater angle, the bigger discharges came about (Hayawi et al., 2009; Saleh and Hiba, 2013). Researched the discharge coefficient and the flow characteristics for a combined hydraulic measuring device of rectangular weir over a semi-round gate. The outcomes showed that the discharge coefficient increment as the head over weir increment and the gate diameter decline. Besides, the distance between the lower edge of weir crest and gate top was the fundamental parameter in the estimation of the discharge coefficient. Shaker and Sarhan (2013) examined the flow over a sharp crested angled weir and under gate in combined structure as flow measurement device. They inferred that the discharge coefficient diminishes with the abatement of angle of inclination. Yaser et al. (2005) utilized the codes of CFD to examine the close and far fields of the flow upstream of orifice and sluice gate. They reasoned that the state of opening exhibited unimportant impact on the upstream flow pattern (Vito, 2000; Matahel, 2001) utilized the Buckingham π-theorem and the fragmented selfsimilarity theory were additionally appropriate to infer head-discharge relationships for simultaneous flow over and under a gate.

The majority of the past investigations were focused on discharge coefficient of combined structures, while few studies were accessible on the downstream local scour. Along these lines, determination of the scour geometry could be helpful to choose the best controlling structure from the perspective on bed stability (Dehghani et al., 2009, 2010; Shahabi et al., 2011). Researched the scour hole characteristics downstream of combined free flow over rectangular weir and underneath gate. They presumed that as the Froude No. increment, the geometry of downstream local scour and sedimentation increment. Yaser et al. (2011) numerically researched the downstream scour of combined weirs and gate model, the results were contrasted with experimental data.

Employing of an orifice with sluice gates, increase the flow discharge with minimizing the horizontal jets under gate that was attributed with higher bed flow velocity and larger scour depth and length downstream these gates, especially in canals of unlined bed. From the previous investigations; gate and orifice might be combined together in one device yielding a simultaneous flow through the orifice and underneath the gate. In this research, a circular orifice employed with sluice gates as a means of energy dissipation downstream the gates was experimentally examined. The fundamental targets of this study were to define the impact of the sluice gate with orifice on the flow pattern and the downstream bed scour. The outcomes were compared with the case of gates with no orifice.

2. Theoretical Analysis

Figure 1 showed definition sketch for the free flow through rounded orifice and below sluice gate of different contraction.

The total discharge through the sluice gate with orifice was calculated as follows:

$$Q_{th} = Q_g + Q_o , \tag{20}$$

where Q_g = Discharge through sluice gate
Q_o = Discharge through rounded orifice
Q_{th} = Total theoretical discharge through the sluice gate with orifice

$$Q_g = GB\sqrt{2gH} \tag{21}$$

$$Q_o = \frac{\pi}{d} d_o^2 \sqrt{2gh} \tag{22}$$

$$Q_{Cact} = c_{OG}\left(GB\sqrt{2gH} + \frac{\pi}{d} d_o^2 \sqrt{2gh}\right) \tag{23}$$

The combined discharge, Q_{Cact} can be written in the following functional form;

$$Q_{Cact} = \phi_1(\rho, \mu, \sigma, B, g, H, h, d_o, G, y_t, S_o) \tag{24}$$

in which ρ: the water density of the flow, μ: the water viscosity, σ: the surface tension, B: the flume width, g: the gravity acceleration, H: the upstream water head (i.e., the gate water head), h: the vertical distance from the orifice center line to the upstream water head (i.e., the orifice water head), d_o: the orifice diameter, G: the gate opening, y_t: the tail gate water depth, and S_o: flume bed slope.

Using the dimensional analysis principles, and considering the viscosity and surface tension were of minor effect. Also, the flume bed slope was kept constant; the following dimensionless form was obtained:

$$c_{OG} = \frac{Q_{Cact}}{GB\sqrt{2gH}} = \phi_2\left(\frac{G}{H}, \frac{d_o}{H}, \frac{h}{H}, \frac{y_t}{H}, \frac{G}{B}, \frac{d_o}{G}\right). \tag{25}$$

3. Experimental Setup

The experimental work was done in a flume at the Hydraulics Research Institute (HRI) of the National Water Research Centre, Egypt. The flume channel was 24.5 m long, 0.74 m wide, 0.70 m depth. A centrifugal pump was used to supply water to the head tank from the capacity tank. The head tank has a gravel box used

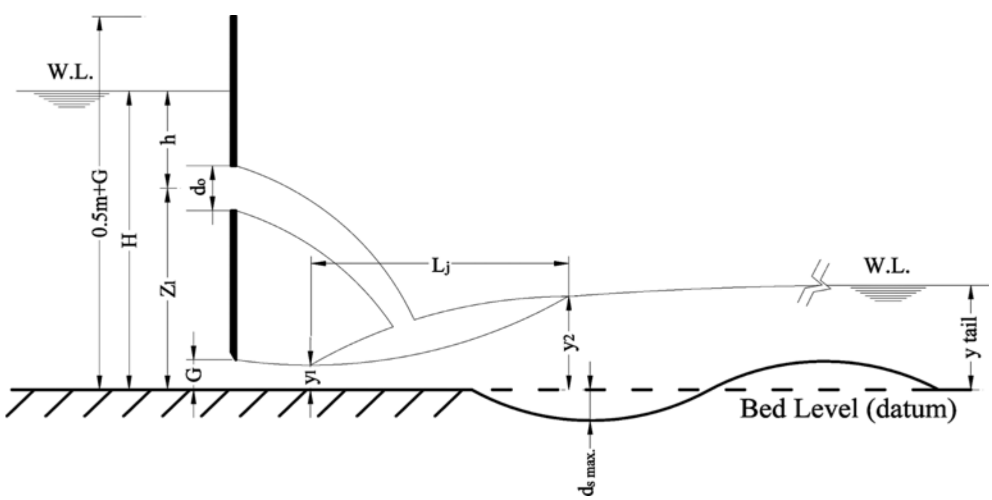

Fig. 1. Definition Sketch for the Sluice Gate with Orifice

Fig. 2. Flow Downstream Sluice Gate with Orifice

to give an even flow allocation over the flume, moreover has compact downstream gate arranged close to the flume end to adjust the downstream water level. Centrifugal pump driven by enlistment motor to re-circle the flow from an underground supply to the flume. The model was a sluice gate made of steel 0.002 m thick, 0.5 m height, and 0.74 m width and related with a rounded orifice was used as a heading-up structure of sluice gate with orifice; Fig. 2.

3.1 Model Set-Up and Measurement Techniques

The test methodology were as per the following: 1) the 0.25 m depth of bed material was set in the flume, and composed to the ideal level; 2) the sluice gate with orifice model was introduced in its place in the flume; 3) the tail gate was totally shut; 4) the flume was loaded up with water all through back feeding until the downstream water depth was accomplished; 5) the pump was gone on to begin upstream water feeding but at a little and cautious behaviour so that there was no underlying scour behind the apron and the filling was done until the water arrives at a depth more prominent than required for desired test; 6) the main gate was opened somewhat more to pass more noteworthy discharge without creating hydraulic jump; 7) the ideal discharge was set and precisely measured utilizing an ultrasonic flow meter with accuracy of ±1%; 8) the tail gate water depth was adjusted by gradually opening the tail gate until the desired tail water depth was accomplished and checked utilizing the point gauge; 9) here the test time begins; 10) following six hours the length of hydraulic jump, and the water surface profile were measured at the longitudinal centreline of the flume using point gauge and levelling device each 5 cm started just downstream the gate and extended to 5 m along the channel; where no appreciable fluctuations in water level were remarked. Moreover, twenty ordinary scales glued to the flume glass side walls at the region of hydraulic jump were used to assure the measurements of the initial and sequent depths; 11) the pump was turned off and the flume was emptied by slanting the tail gate gradually not to disturb the bed; 12) the bed levels were recorded. The past stages were rehashed for each run.

3.2 Run Duration

The experiments were executed under clear-water condition applying different hydraulic parameters. So as to estimate the necessary time to accomplish equilibrium state, i.e., at the point when the maximum scour depth was around time invariant, the primarily experiments were performed for 360 minutes. As practically 90% of the maximum scour depth was accomplished past the 120 minutes; the 360 minutes were sufficient enough.

4. Model Runs

The test program comprises of 45 test runs using, 3 discharges, 3 upstream water heads, 5 orifice diameters, and 7 tail gate water depths. The extents of the used factors were presented in Table 1. The scenarios were completed to explore the impact of the previous variables on the downstream flow pattern also the bed topography bookkeeping the contraction scour depth.

5. Results and Discussions

The outcomes were exhibited regarding flow characteristics notwithstanding the downstream bed configurations. The results of the flow pattern were emphasized on relation between the gate opening and the orifice areas under various flow conditions, the

Table 1. Range of Variables Used in the Experiments

Parameter	Symbol	Value	Range		Units
			From	To	
Discharge	Q	35, 40, 45	35	45	l/s
Upstream water head	H	32.5, 32.7, 40.85	32.5	40.85	cm
Orifice diameter	d_o	0, 6, 8, 12, 14	0	14	cm
Height of gate opening above bed	G	1.5, 1.6, 1.9, 2.4, 2.6, 2.8, 3, 3.6, 3.8	1.5	3.8	cm
Height of orifice center above bed	Z_1	26.5, 26.6, 26.9, 27.4, 27.6, 27.8, 28.0, 28.6, 28.8	26.5	28.8	cm
Tail gate water depth	y_t	11.5, 12, 12.5, 13, 13.5, 14, 14.5	11.5	14.5	cm

discharge coefficient, characteristics of the hydraulic jump, and the energy scattering in the jump. However, the bed configurations were introduced as far as the scour depth.

5.1 The Discharge Coefficient

The flow through the orifice and under the sluice gate, consequently to keep the discharge and upstream water head consistent; as the area of gate opening increment, the orifice area should be diminished; Fig. 3. The indicated relationship wasn't unadulterated straight because of the impact of the discharge coefficient. Besides, it was seen that under fixed orifice area, the gate area incremented as the upstream Froude No. declined. That in light of the fact that the flow of lower Froude No. implied high upstream water depth that required more gate area than the flow of higher Froude No.

To explore the discharge coefficient of the sluice gate with orifice contrasted with the conventional sluice gate; Fig. 4 was plotted. Excluding the outcomes of Henderson (1966) it was seen that the discharge coefficient was less sensitive to the orifice installation contrasted with the gate opening; as the measured discharge coefficients for the sluice gate with orifice were close the conventional sluice gate. Likewise, it was noticed that the maximum discharge coefficient for the sluice gate with orifice was located at the minimum upstream Froude No. That can be clarified under fixed gate opening and orifice diameter, expanding the upstream water head implied increase in the upstream

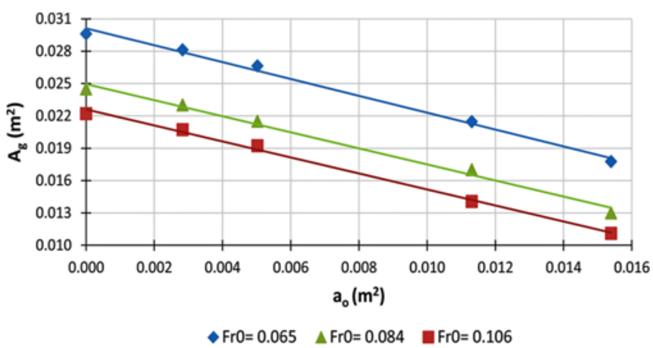

Fig. 3. Relation between Orifice and Gate Areas under Different Flow Conditions

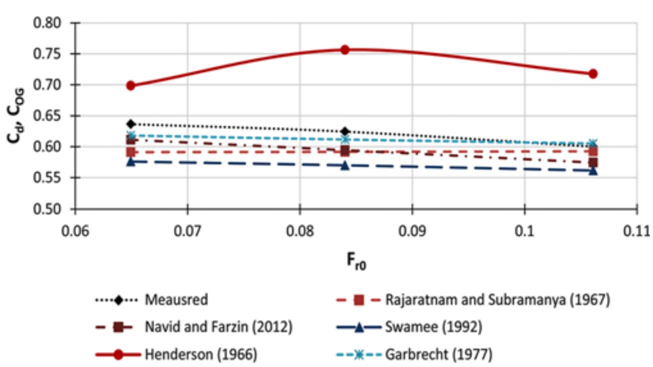

Fig. 4. The Discharge Coefficient for the Sluice Gate with Orifice Compared to Other Studies

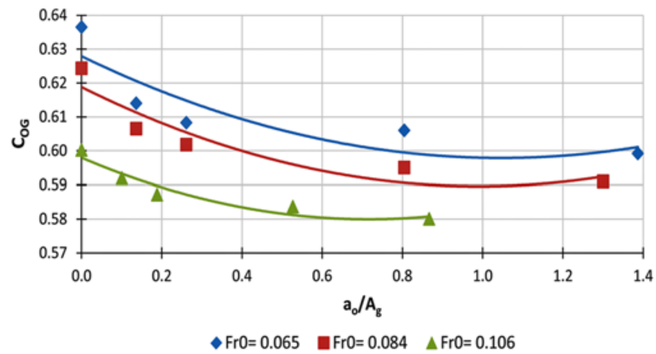

Fig. 5. Relation between the Discharge Coefficient and Areas of Orifice over Gate

hydrostatic pressure that enforced the flow to go through the small openings of the orifice and the gate, accordingly the coefficient of contraction $\left(\frac{y_1}{G}\right)$ declined and the discharge coefficient as well.

Figure 5 was plotted to clarify the impact of orifice diameter on the discharge coefficient for various upstream Froude numbers. The figure demonstrated the discoveries displayed in Fig. 4; where the discharge coefficient was conversely corresponding to the upstream Froude No. regardless the orifice diameter. But due to the difficulties faced the flow to pass a circular opening; the discharge coefficient for an orifice was less than a gate of the similar area. Consequently, the discoveries of Fig. 5 were for unchanged Froude. No., the discharge coefficient was diminished as the area ratio between the orifice and the gate opening $\left(\frac{a_o}{A_g}\right)$ increment was reasonably displayed.

5.2 The Hydraulics and Flow Attributes

5.2.1 Influence of the Sluice Gate with Orifice on the Characteristics of Hydraulic Jump

Figure 6 indicated the hydraulic jump length at various proportions of orifice and gate areas under fixed 12.5 cm tail gate water depth. It was seen that for consistent upstream Froude No., the minimum jump length was situated at $\left(\frac{a_o}{A_g}=0\right)$; where no orifices

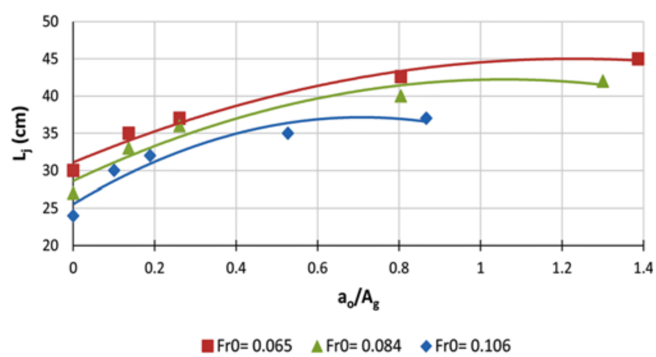

Fig. 6. Relation between the Jump Length and Areas of Orifice over Gate

were introduced and the sluice gate with orifice acted as conventional sluice gate. However, the jump length reached out to increment straightforwardly as the orifice area increment. That can be delineated by assessing the comments displayed in Fig. 3; where the region underneath the sluice gate with orifice was contrarily relative to the orifice area, subsequently the jump length increment. Underlining the upstream Froude No., the figure displayed for steady $\left(\frac{a_o}{A_g}\right)$, the jump length was contrarily corresponding to the upstream Froude No. Where the lower upstream Froude No. the higher upstream hydrostatic head, subsequently the longer jump length.

To examine the impact of the sluice gate with orifice on the conjugate depths of the hydraulic jump; Fig. 7 was plotted. For the occurrence of no orifice where $\left(\frac{a_o}{A_g}=0\right)$, the proportion between the initial depth and the sequent depth i.e., $\left(\frac{y_1}{y_2}\right)$ was maximum notwithstanding the flow conditions. The purposes for that were as on account of no orifice, the gate opening was expanded to enable more flow to pass unreservedly, thus the initial depth was expanded. And afterward introducing an orifice despite its diameter, the estimation of $\left(\frac{y_1}{y_2}\right)$ was tragically diminished up to $\left(\frac{a_o}{A_g}=0.16\right)$ which spoke to the defining moment of the figure; where the more increment in orifice diameter showed unnoticeable impact on the conjugate depths.

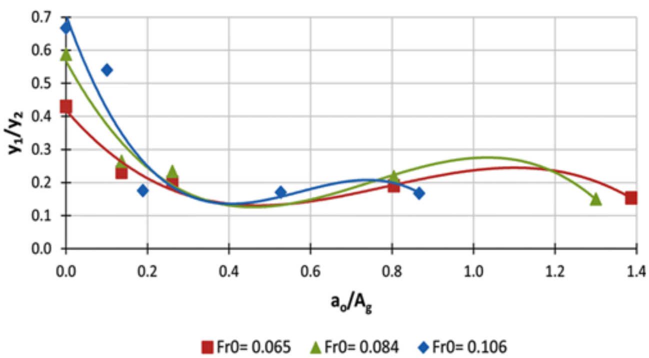

Fig. 7. Relation between the Conjugate Depths and Areas of Orifice over Gate

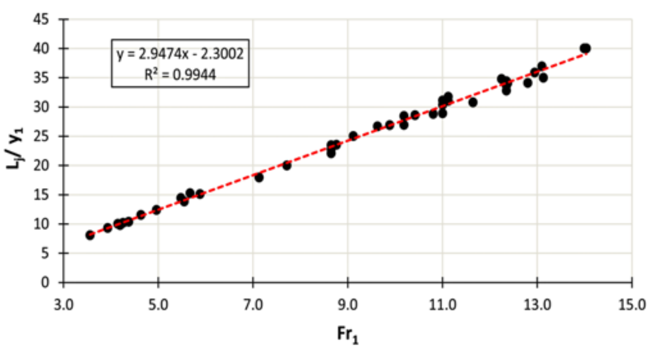

Fig. 8. Relation between the Jump Characteristics and the Froude No. at the Initial Depth

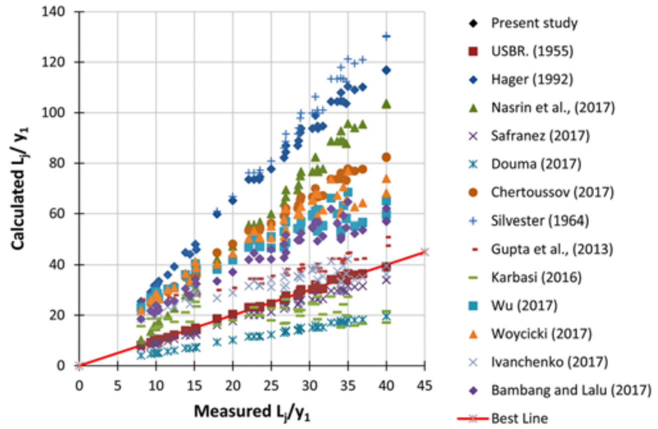

Fig. 9. Comparison between Measured and Calculated Jump Lengths

Figure 8 showed the relation between the Froude No. at the initial depth and the jump attributes exhibited as far as the proportion between the jump length and the initial depth i.e., $\left(\frac{L_j}{y_1}\right)$ for all tests executed in this study. The figure featured the direct linear relationship between the exhibited factors despite orifice installation at any diameter. That can be shown by the decline of initial depth, both Froude No. at the initial depth (F_{r1}) and jump length (L_j) were expanded regardless orifice installation.

The results of applying existed equations utilized to appraise the jump length downstream a conventional sluice gate were contrasted with the measured jump length downstream the sluice gate with orifice in this investigation; to explore the adequacy of these equations to be applied for prediction of jump length downstream sluice gate with orifice; Fig. 9 was plotted. The measured jump lengths were contrasted with 13 unique equations presented in section 1. The figure displayed that solitary the equations introduced by (USBR, 1955; Safranez, 2017) can be applicable for the prediction of the jump length downstream sluice gate with orifice, gave that $\frac{a_o}{A_g} \le 1.4$, and $3.55 \le F_{r1} \le 14.03$. Where, the percentage of errors between the average measured jump lengths contrasted with the lengths determined by (USBR, 1955; Safranez, 2017) were 3.18% and 9.35%, separately.

5.2.2 Influence of the Sluice Gate with orifice on the Energy Dissipation

The dispersed energy in the hydraulic jump downstream the sluice gate with orifice was brought about by the impact of the upward flow from the gate with the close to surface free spill out of the orifice. The energy dissemination exhibited in the Figs. 10 and 11 was communicated as a percentage of $\frac{\Delta E}{E_1}$, where ΔE was the energy differences at the sequent and the initial depths respectively (i.e., $E_2 - E_1$).

To talk about the impact of orifice installation on energy dissemination, Figs. 11 and 7 should be gathered side by side; where similar curves trend were seen yet in a reversed direction.

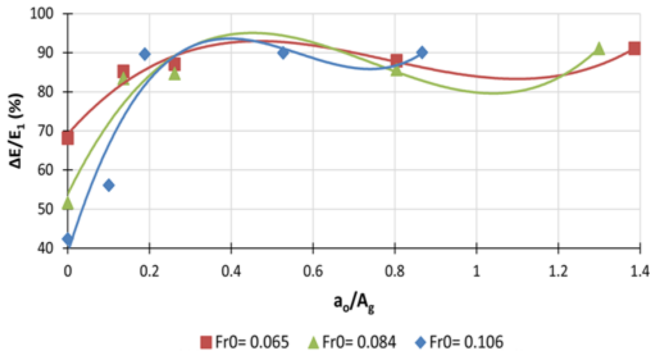

Fig. 10. Relation between the Energy Dissipation and Areas of Orifice over Gate

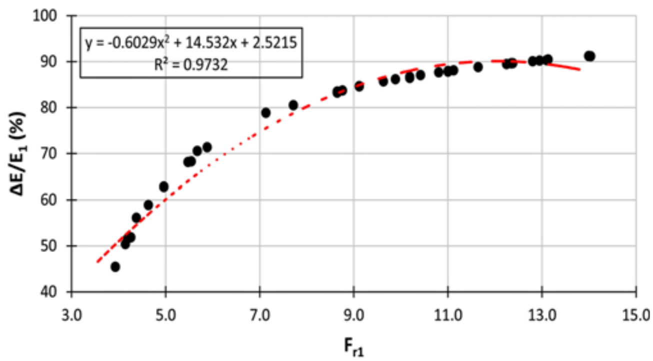

Fig. 11. Relation between the Energy Dissipation and the Froude No. at the Initial Depth

For the instance of no orifices installation; Fig. 11 showed that the rate of energy dispersal was expanded by the decrease of the upstream Froude No. The reasons were investigated and discussed in Fig. 7 as the higher upstream Froude No. had approximated values for the conjugate depths; thus the energy scattering was unnoticeable. Then again as was seen in Fig. 7, nevertheless the upstream Froude No., installing an orifice to the sluice gate discernibly expands the energy dissemination up to $\frac{a_o}{A_g} = 0.16$ at which the energy dispersal was extensive, at that point the energy scattering esteems would in general be fixed even the $\frac{a_o}{A_g}$ was expanded.

Figure 11 was plotted to investigate the impact of the Froude No. at the initial depth on the energy dissemination for all tests in this investigation. It was seen that notwithstanding to orifice installation, the rate of energy dispersal was expanded as the Froude No. at the initial depth increment. The figure showed that for flow condition of $3.9 \leq F_{r1} \leq 7.1$ (i.e., 82.05% increase in F_{r1}) the rate of energy dissemination was remarkable and expanded by 73.5%. However, for $8.6 \leq F_{r1} \leq 14$ (i.e., 62.79% increase in F_{r1}) the rate of energy scattering was less affected by the Froude No. at the initial depth and increased by 9.204%. Henceforth, it tended to be reasoned that, the energy dispersal was significant downstream the sluice gate with orifice for the occasion of $F_{r1} \leq 7.1$.

Table 2. Characteristics of Bed Material

d_{10} (mm)	d_{16} (mm)	d_{50} (mm)	d_{60} (mm)	d_{84} (mm)	C_u	σ_g
0.214	0.246	0.485	0.576	0.885	2.692	1.896

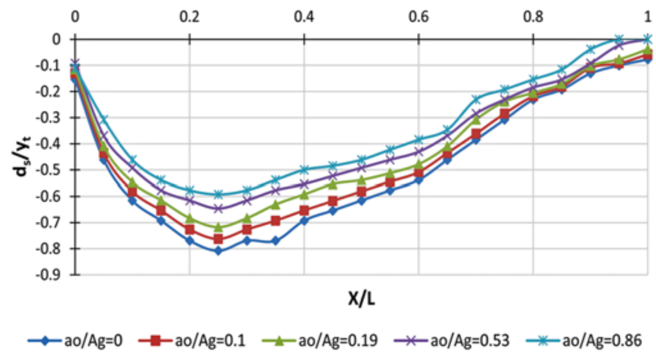

Fig. 12. Effect of Opening Areas on the Scour Depth

5.2.3 The Bed Configurations

A bed material of 0.25 m depth, 2.0 m length filling the flume width were independently used. Sieve size distribution tests were done to describe the material properties and the outcomes were laid out in Table 2.

A planned mesh comprised of 189 measuring points for bed profile readings. The points were organized in 9 lines and 21 segments. The first row took place exactly at the left flume wall. The spacing between lines were 10 cm with the exception of the last line has 4 cm separating to cover the flume width. The sections were begun just by the apron end and covered 2 m length of bed material with 10 cm interims.

Figure 12 was exhibited to investigate the impact of orifice diameter on the downstream local scour. The figure was plotted under fixed upstream Froude No., discharge, upstream and tail gate water depths of 0.106, 45 l/s, 32.7 cm, and 13 cm, individually. The figure outlined that the impact of orifice diameter on the location of greatest scour depth was irrelevant; as it stayed consistent and situated at $\frac{x}{L} = 0.25$; where X: the distance from apron end to any point along bed material, and L: the total length of bed material. However, the orifice diameter demonstrated remarkable impact on the values of maximum scour depth; where at consistent $\frac{x}{L}$ it was seen that as the value of $\frac{a_o}{A_g}$ increment, the greatest scour depth was perceptibly diminished. That can be delineated as the orifice diameter increment; more flow was permitted to pass downward to crash the upward flow downstream the sluice gate causing more energy scattering, and thusly decrease in bed unsettling influence. The figure underlined that utilizing a sluice gate with orifice of $\frac{a_o}{A_g}$ = 0.1, 0.19, 0.53, and 0.86 diminished the maximum scour depth by 5.6%, 11.2%, 20%, and 26.6%, separately contrasted with a conventional sluice gate without orifice. In spite of the fact that orifice installation was significantly influencing the local scour depth yet its impact

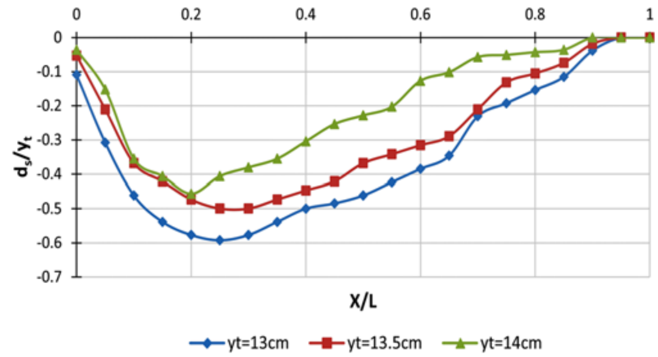

Fig. 13. Effect of Tail Gate Water Depth on the Scour Depth

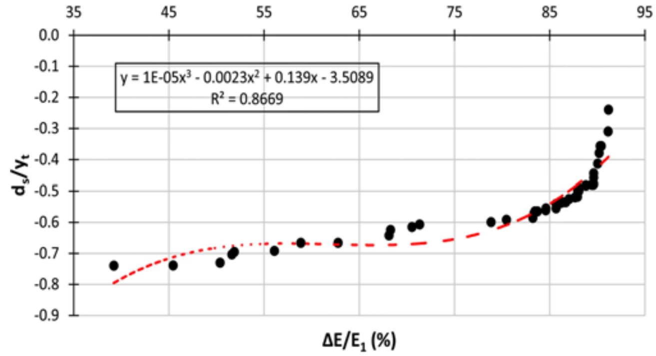

Fig. 14. Relation between the Energy Dissipation and the Maximum Scour Depth

on scour length was unremarkable; where the scour length devoured the absolute length of bed material under the examination. Extraordinary special case was seen for the instance of $\frac{a_o}{A_g}=0.86$, where the scour length was 5% less than any other case.

To investigate the impact of tail gate water depth on the downstream local scour depth; Fig. 13 was plotted. The figure was introduced for a sluice gate with orifice model of $\frac{a_o}{A_g}=0.86$ under steady upstream Froude No., discharge, upstream water depth of 0.106, 45 l/s, and 32.7 cm, respectively. The tested tail gate water depths were 13, 13.5, and 14 cm. The figure reasoned that the bed configurations were diminished as the tail gate water depth increment. Where, the maximum scour depth was decreased by 15.64% and 22.94% for 13.5 cm and 14 cm tail gate water depths, respectively compared to 13 cm tail gate water depth. That can be outlined, as the tail gate water depth increased; the downstream hydrostatic head increment and the hydraulic jump was faced by a massive block of water. Thusly, extensive energy dispersal and lower bed configurations were pronounced.

To characterize the relation between the energy dissipation and the local maximum scour depth; Fig. 14 was exhibited for the tests run in this investigation. It was commented that the scour depths were decline by the expansion of the energy dispersal. However, the figure might be isolated along with two zones; where the line of separation was $\frac{\Delta D}{E_1}=75\%$. On account of $39.21\% < \frac{\Delta E}{E_1} < 71.33\%$ (i.e., 81.91% increase in energy dissipation), the $\frac{d_s}{y_t}$ was decreased by 17.97%. However, for $78.84\% < \frac{\Delta E}{E_1} < 91.16\%$ (i.e., 15.62% increase in energy dissipation), the $\frac{d_s}{y_t}$ was decreased by 60%. Henceforth, the sluice gate with orifice adequately decreased the downstream bed disturbance provided that $\frac{\Delta E}{E_1}\geq 75\%$.

The test results were utilized for corresponding the different dimensionless variables to create empirical formulae for calculation the discharge coefficient, jump length, and the downstream scour depth for sluice gate with orifice. With the assistance of nonlinear regression analysis, the accompanying observational recipes were inferred:

$$C_{OG}=\exp\left[-0.983F_{ro}-0.002F_{r1}-0.011\left(\frac{a_0}{A_f}\right)+0.00014\left(\frac{H}{G}\right)+0.0051\left(\frac{H}{h}\right)+0.0056\left(\frac{H}{y_t}\right)+0.672\right], \quad (26)$$

$$\frac{L_j}{G}=\exp\left[-21.877F_{ro}+0.656F_{r1}+4.904\left(\frac{a_0}{A_g}\right)+0.439\left(\frac{H}{G}\right)+0.0079\left(\frac{H}{h}\right)-1.382\left(\frac{H}{y_t}\right)+5.986\right], \quad (27)$$

$$\frac{d_s}{G}=\exp\left[57.472F_{ro}+0.0774F_{r1}-0.992\left(\frac{a_0}{A_g}\right)+0.299\left(\frac{H}{G}\right)+0.349\left(\frac{H}{h}\right)+3.589\left(\frac{H}{y_t}\right)-16.15\right]. \quad (28)$$

The accuracy of these equations was tested using the statistical performance indices presented in Table 3 and found to be in the acceptable range. Moreover, Fig. 15 was plotted to compare the measured and predicted values to give more confidence in the developed equations. The outcomes demonstrated that the percentage of errors were found

Table 3. Statistical Model Evaluation

Equation number	Coefficients of determination (R^2)	Sum of squared residuals (SSR)	Standard error of the estimate (SSE)	Durbin Watson Statistic DW
26	0.793	2.32	0.216	2.72
27	0.995	7.28	0.438	2.01
28	0.918	4.58	0.362	2.11

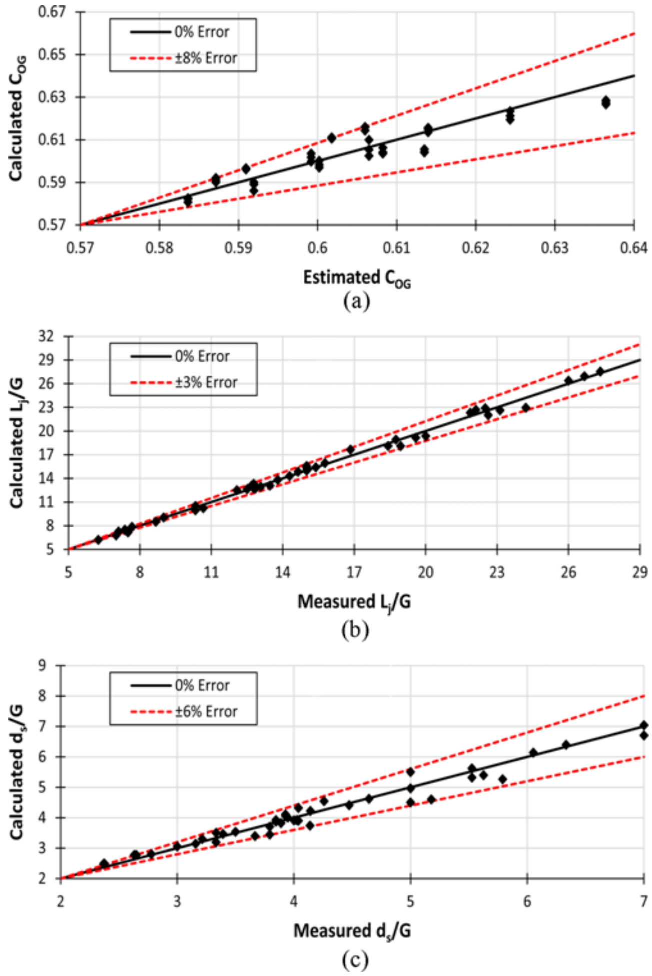

Fig. 15. Comparison between Measured and Predicted Values for: (a) The Discharge Coefficient, (b) Dimensionless Jump Length, (c) Dimensionless Scour Depth

between 3% and 8%.

The equations were valid for the following conditions: $0.06 \le F_{r0} \le 0.103$; $3.55 \le F_{r1} \le 14.03$; $0 \le \frac{a_o}{A_g} \le 1.38$; $8.16 \le \frac{H}{G} \le 27.23$; $2.57 \le \frac{H}{h} \le 4.33$; $2.33 \le \frac{H}{y_t} \le 3.03$.

The derived formulas inferred that the upstream Froude No. (F_{ro}) was the dominant parameter that influenced the hydraulics and bed configurations downstream the sluice gate with orifice. Underlining on Eq. (26) it was discovered that all referenced variables demonstrated insignificant impact on the discharge coefficient of the sluice gate with orifice except the upstream Froude No. (F_{ro}) that was conversely relative to the discharge coefficient which affirmed the discoveries of Fig. 4. Eq. (27) showed that the jump length was legitimately corresponding to $\frac{a_o}{A_g}$ which confirmed the discoveries of Fig. 6. Focusing on the downstream scour depth, Eq. (28) exhibited that the scour depth were expanded as the upstream Froude No. (F_{ro}) increment and diminished as the $\frac{a_o}{A_g}$ increment; thusly assured the conclusions of Fig. 12.

6. Conclusions

Employing of an orifice with sluice gates increased the flow discharge with minimizing the horizontal jets under gates. In this research, a circular orifice was employed with sluice gates as a means of energy dissipation downstream these gates, was experimentally investigated. The flow pattern and the bed configurations downstream sluice gate with orifice were evaluated and the following conclusions were drawn:

1. Installing an orifice to a conventional sluice gate dissipated the jump energy and minimized the downstream bed configurations.
2. For constant upstream Froude No., the orifice area increased as the gate area decreased.
3. The installed orifice has a small influence on the discharge coefficient compared to the effect of gate opening.
4. For fixed gate opening and orifice diameter, the discharge coefficient was contrarily corresponding to the upstream Froude No.
5. The discharge coefficient decrease as the value of $\left(\frac{a_o}{A_g}\right)$ decrease at constant flow conditions.
6. Although, the lower sensitivity to orifice effect compared to the underneath opening, the jump length was inversely proportional to orifice diameter at constant flow conditions. This approved that orifice with sluice gated decreases the hydraulic jump length.
7. To lessen the jump height downstream the sluice gate with orifice and make the optimum use for orifice installation from the view of energy dissipation, the accompanying condition should be fulfilled $\left(\frac{a_o}{A_g} \ge 0.16\right)$.
8. Regardless to orifice installation and its diameter, the jump length was expanded by the decline of the initial water depth.
9. The equations presented by (USBR, 1955; Safranez, 2017) can be used for the prediction of jump length downstream the sluice gate with orifice with a limitation to parameters of ($\frac{a_o}{A_g} \le 1.4$, and $3.55 \le F_{r1} \le 14.03$).
10. The rate of energy dissipation was legitimately corresponding to the Froude No. at the initial water depth regardless to orifice installation.
11. The sluice gate with orifice successfully improved the energy dissipation on account of $F_{r1} \le 7.1$.
12. Utilizing sluice gate with orifice of $\left(\frac{a_o}{A_g} = 0.86\right)$ exhibited the minimum downstream bed changes in terms of local scour depth and length.
13. Regardless the orifice diameter, the bed configurations were conversely relative to the tail gate water depth.
14. The scour depths were decreased by the increase of the

downstream energy dissipation.

15. The sluice gate with orifice efficiently reduces the downstream bed disturbance provided that, ($\frac{\Delta E}{E_1} \geq 75\%$).

Acknowledgments

This work was completed at the Hydraulic Research Institute (HRI), the National Water Research Centre (NWRC), Egypt. The authors present their appreciation to all members and specialists in the (HRI) for their help and encourage.

Nomenclature

A_g = Area of gate opening [m^2]
a_o = Area of orifice [m^2]
B = Flume width [m]
B' = Divergence ratio
C_d = Discharge coefficient for the sluice gate
C_j = Hydraulic jump length coefficient
c_{OG} = Discharge coefficient for the sluice gate with orifice
C_u = Uniformity coefficient
d_o = The orifice diameter [m]
d_s = Maximum scour depth [m]
E_1 = Energy at the initial depth [m]
E_2 = Energy at the sequent depth [m]
F_{ro} = Upstream Froude No.
F_{r1} = Froude No. at the initial depth
g = Gravitational acceleration [m/s^2]
H = Upstream water head [m]
h = The vertical distance from the orifice center line to the upstream water head [m]
L = Length of bed material [m]
L_j = Length of hydraulic jump [m]
Q_{Cact} = The combined discharge [L/s]
Q_g = Discharge through a sluice gate [L/s]
Q_o = Discharge through a rounded orifice [L/s]
Q_{th} = Total theoretical discharge through sluice gate with orifice [L/s]
r = Height of roughness elements [m]
R_{e1} = Reynolds number at the initial depth
S_o = Flume bed slope
V = The mean flow velocity [m/s]
X = The distance from apron end to any point along bed material [m]
y_1 = Initial depth of the hydraulic jump [m]
y_2 = Sequent depth of the hydraulic jump [m]
y_t = Tail gate water depth [m]
ΔE = Energy difference [m]
μ = Dynamic viscosity of water [kg/m.s]
ρ = Water density of the flow [kg/m^3]
σ = Surface tension of water [N/m]
σ_g = Geometric standard deviation of the grain size distribution

ORCID

Ibrahim M. Mohamed https://orcid.org/0000-0003-3168-6626
Fahmy S. Abdelhaleem https://orcid.org/0000-0002-3279-9668

References

Alhamid AA (1999) Analysis and formulation of flow through combined V-notch-gate-device. *Journal of Hydraulic Research* 37(5):697-705, DOI: 10.1080/00221689909498524

Alhamid A, Husain D, Negm A (1996) Discharge equation for simultaneous flow over rectangular weirs and below inverted triangular weirs. *Arab Gulf Journal of Scientific Research* 14(3):595-607

Alhamid A, Negm A, Al-Brahim AM (1997) Discharge equation for proposed self-cleaning device. *Journal of King Saud University, Engineering Science, Riyadh, Saudi Arabia* 9(1):13-24, DOI: 10.1016/S1018-3639(18)30664-0

Bambang S, Lalu M (2017) Study of hydraulic jump length coefficient with the leap generation by canal gate model. *American Journal of Civil Engineering* 5(3):148-154, DOI: 10.11648/j.ajce.20170503.14

Carlos S, Manuel G, José R (2009) Benchmark of discharge calibration methods for submerged sluice gates. *Journal of Irrigation and Drainage Engineering* 135:676-682, DOI: 10.1061/(ASCE)IR.1943-4774.0000013

Carollo FG, Ferro V, Pampalone V (2009) New solution of classical hydraulic jump. *Journal of Hydraulic Engineering* 135:527-531, DOI: 10.1061/(ASCE)HY.1943-7900.0000036

Chertoussov, 1935 in Thandaveswara (2017) Hydraulics course material. Section 29.5. NPTEL, Acceced January 8, 2017, https://nptel.ac.in/courses/105106114/pdfs/Unit29/29_5.pdf.

Dehghani A, Bashiri H, Dehghani N (2010) Downstream scour of combined flow over weirs and below gates. Proceedings of the international conference on fluvial hydraulics, September 8-10, Braunschweig, Germany

Dehghani A, Bashiri H, Meshkati S, Mohamad E, Ahadpour A (2009) Experimental investigation of scouring in downstream of combined flow over weirs and below gates. 33rd IAHR conference, August 9-14, Vancouver, Canada

Delwar H (1999) Dynamic study of simultaneous underflow-overflow past low head sluice gates. *Journal of King Saud University, Engineering Science, Riyadh, Saudi Arabia* 11(1):51-67

Douma, 1934 in Thandaveswara (2017) Hydraulics course material. Section 29.5. NPTEL, Acceced January 8, 2017, https://nptel.ac.in/courses/105106114/pdfs/Unit29/29_5.pdf.

Garbrecht G (1977) Discussion of 'Discharge computations at river control structures' by L. Dannie. *Journal of the Hydraulics Division* 103(12):1481-1484

Gupta SK, Mehta R, Dwivedi V (2013) Modeling of relative length and relative energy loss of free hydraulic jump in horizontal prismatic channel. *Procedia Engineering* 51:529, DOI: 10.1016/j.proeng.2013.01.075

Hager WH (1992) Energy dissipators and hydraulic jump. Springer Science and Business Media, Berlin, Germany, 8

Hayawi H, Hayawi G, Amal A (2009) Coefficient of discharge for a combined hydraulic measuring device. *Al-Rafidain Engineering Journal* 17(6):92-100, DOI: 10.33899/rengj.2009.43616

Hayawi H, Yahia A, Hayawi A (2008) Free combined flow over a triangular weir and under rectangular gate. *Damascus University Journal* 24:9-22

Henderson FM (1966) Open channel flow. Macmillan, New York, NY, USA, 202-210

Ivanchenko, 1935 in Thandaveswara (2017) Hydraulics course material. Section 29.5. NPTEL, Acceced January 8, 2017, https://nptel.ac.in/courses/105106114/pdfs/Unit29/29_5.pdf.

Jamal M, Samani M (2009) Combined flow over weir and under gate. *Journal of Hydraulic Engineering* 135(3), DOI: 10.1061/(ASCE)0733-9429(2009)135:3(224)

Karbasi M (2016) Estimation of classical hydraulic jump length using teaching–learning based optimization algorithm. *Journal of Materials and Environmental Science* 7(8):2947-2954

Leutheusser H, Kartha V (1972) Effects of inflow conditions on hydraulic jump. *Journal of the Hydraulics Division* 98(8):1367-1385

Majcherek H (1984) Submerged discharge relations of logarithmic weirs. *Journal of Hydraulic Engineering* 110(6):840-846, DOI: 10.1061/(ASCE)0733-9429(1984)110:6(840)

Matahel A (2001) Simultaneous flow over and under a gate. *Journal of Irrigation and Drainage Engineering* 127(5):325-328, DOI: 10.1061/(ASCE)0733-9437(2001)127:5(325)

McCorquodale JA, Khalifa A (1983) Internal flow in hydraulic jumps. *Journal of Hydraulic Engineering* 109:684-701, DOI: 10.1061/(ASCE)0733-9429(1983)109:5(684)

Nasrin H, Ali H, Davod F, Carlo G (2017) An experimental study of hydraulic jump in a gradually expanding rectangular stilling basin with roughened bed. *Water* 9(12), DOI: 10.3390/w9120945

Negm A (1996) Discharge prediction model for simultaneous underflow-overflow. Proceedings of the 6th international symposium, September 8-10, Tallahassee, FL, USA, 665-670

Negm AM (2002) Discussion: Analysis and formulation of flow through combined v-notch-gate-device by Abdelaziz A. Alhamid, Journal of Hydraulic Research, Vol. 37, No. 5, pp. 697-705. *Journal of Hydralic Research* 40(6):755-765, DOI: 10.1080/00221680209499922

Negm A, Al-Brahim A, Alhamid A (2002) Combined-free flow over weirs and below gate. *Journal of Hydraulic Research* 40(3):359-365, DOI: 10.1080/00221680209499950

Negm A, El-Saiad A, Alhamid A, Husain D (1994) Characteristics of simultaneous flow over weir and below inverted V-notches. *Civil Engineering Research Magazine, Faculty of Engineering, Al-Azher University, Cairo, Egypt* 16(9):786-799

Oskuyi N, Salmasi F (2012) Vertical sluice gate discharge coefficient. *Journal of Civil Engineering and Urbanism* 2(3):108-114

Rajaratnam N (1977) Free flow immediately below sluice gate. *Journal of Hydraulic Engineering Division* 103(4):345-351

Rajaratnam N, Subramanya K (1967) Flow equation for the sluice gate. *Journal, Irrigation and Drainage Division Engineering* 93(3):167-186

Safranez, 1933-39 in Thandaveswara (2017) Hydraulics course material. Section 29.5. NPTEL, Acceced January 8, 2017, https://nptel.ac.in/courses/105106114/pdfs/Unit29/29_5.pdf.

Saleh IK, Hiba A (2013) Study the free flow over compound weir and below semi circular gate. *International Journal of Scientific & Engineering Research* 4(10):1486-1491

Shahabi M, Talebbeydokhti N, Dehghani A, Telvari A, Rakhshanderoo G (2011) Experimental investigation of the effect of contraction on scouring in downstream of combined flow over weirs and below gate. 5th SASTech, Khavaran Higher-Education Institute, Mashhad, Iran, Accessed May 12-14, 2011, https://www.civilica.com/Paper-SASTECH05-SASTECH05_060.html

Shaker AJ, Sarhan A (2013) Experimental study of combined oblique weir and gate structure. *ARPN Journal of Engineering and Applied Sciences* 8(4):306-315

Silvester R (1964) Hydraulic jump in all shapes of horizontal channels. *Journal of the Hydraulics Division* 90:23

Swamee P (1992) Sluice-gate discharge equations. *Journal of Irrigation and Drainage Engineering* 118(1):56-60, DOI: 10.1061/(ASCE)0733-9437(1992)118:1(56)

USBR (1955) Research studies on stilling basins, energy dissipators and associated appurtenances. Hydraulic Laboratory Report Volume 399, Washington DC, USA, 393-438

Vito F (2000) Simultaneous flow over and under a gate. *Journal of Irrigation and Drainage Engineering* 126(3):190-193, DOI: 10.1061/(ASCE)0733-9437(2000)126:3(190)

Woycicki, 1931 in Thandaveswara (2017) Hydraulics course material. Section 29.5. NPTEL, Acceced January 8, 2017, https://nptel.ac.in/courses/105106114/pdfs/Unit29/29_5.pdf.

Wu, 1949 in Thandaveswara (2017) Hydraulics course material. Section 29.5. NPTEL, Acceced January 8, 2017, https://nptel.ac.in/courses/105106114/pdfs/Unit29/29_5.pdf.

Yaser S, David Z, Nallamuthu R (2005) Flow upstream of orifices and sluice gates. *Journal of Hydraulic Engineering* 131(2):127-133, DOI: 10.1061/(ASCE)0733-9429(2005)131:2(127)

Yaser SG, Mojtaba S, Sirous E (2011) Three-dimension numerical simulation of scour temporal changes due to flow in the downstream of combined weirs and gate model. *Civil Engineering Journal* 3(11):1111-1120, DOI: 10.28991/cej-030941